Thin Solid Films 717 (2021) 138469

Contents lists available at ScienceDirect

Thin Solid Films

journal homepage: www.elsevier.com/locate/tsf

Structure, electronic and optical properties of chalcopyrite semiconductor $AgTiX_2$ (X = S, Se, Te): A density functional theory study

Prabhat Ranjan [a,*], Pancham Kumar [b], Praveen K. Surolia [c], Tanmoy Chakraborty [d,*]

[a] Department of Mechatronics Engineering, Manipal University Jaipur, Dehmi kalan, Jaipur-303007, India
[b] School of Electrical Skills, Bhartiya Skill Development University, Jaipur-302042, India
[c] Department of Chemistry, Manipal University Jaipur, Dehmi kalan, Jaipur-303007, India
[d] Department of Chemistry and Biochemistry, School of Basic Sciences and Research, Sharda University, Greater Noida-201310, India

ARTICLE INFO

Keywords:
Chalcopyrite semiconductor
Silver titanium selenide
Density functional theory
Solar cells
Highest occupied molecular orbital- lowest unoccupied molecular orbital

ABSTRACT

The structure, electronic and optical properties of chalcopyrite-type semiconductor material $AgTiX_2$ (X = S, Se, Te) are investigated invoking Density Functional Theory (DFT). The computed Highest Occupied Molecular Orbital (HOMO)-Lowest Unoccupied Molecular Orbital (LUMO) energy gap of $AgTiX_2$ molecule with and without 4f function on Ag is in the range of 2.319 eV – 3.211 eV and 2.092 eV – 3.056 eV respectively. It establishes that $AgTiX_2$ can be used as potential candidate for optoelectronic and photovoltaic applications, especially in solar cells. Result analysis reveals that $AgTiS_2$, having a rectangular geometry with C_{2v} point group and doublet spin multiplicity, is the most stable system with maximum HOMO-LUMO gap. Our calculated DFT based global descriptors and spectral analysis transpires that HOMO-LUMO energy gap, harmonic frequency and intensity of IR and Raman spectra decreases from $AgTiS_2$ to $AgTiSe_2$ to $AgTiTe_2$. A strong correlation is established between DFT based global descriptors and HOMO-LUMO gap from this analysis.

1. Introduction

In recent years, the study of chalcopyrite semiconductor materials has received a significant attention due to its potential applications in thin film solar cells, optical emitter and optical absorber and photocatalysts [1–9]. The main feature of chalcopyrite semiconductor is that they have unique electronic and optical properties and large transparency range of visible and infrared spectra [10]. Ternary compounds of $A^{I}B^{III}C_2^{VI}$ semiconductor group have a direct band gap and high adsorption coefficient under sunlight [11–13]. Chalcopyrite semiconductors are suitable for the realization of p-n hetero-junction with semiconductor group II-VI due to their similarity in structure [14]. Chalcopyrite semiconductors are divided into two classes, Cu-based and Ag-based chalcopyrite compounds. Cu-based chalcopyrite materials are studied extensively due to its interesting physico-chemical properties like high absorption coefficient and appropriate optical band gap which is suitable for the construction of thin film solar cells [15]. Recently, we have also studied Cu-based chalcopyrite-type materials, $CuTiX_2$ (X = S, Se, Te) by using Density Functional Theory (DFT) approach and found that the energy gap of these compounds are in the range of 2.40 eV to 3.19 eV [16].

The Ag-based chalcopyrite-type materials have potential technological applications in non-linear optical devices, photonic sensors, light emitting diode and photovoltaics [1,15,17-20]. The silver-based chalcopyrite compound has a particular valence band structure which displays different polarization-dependent optical property than the Cu-based chalcopyrite-type materials [21]. It indicates that Ag-based chalcopyrite materials may be suitable for detection of linearly polarized lights [1]. The compound $AgGaSe_2$ and $AgGaS_2$ have a direct band gap of 1.82 eV to 2.7 eV respectively and good transparency over 500–1200 nm wavelength [17–19]. Ho et al. [1] found that chalcopyrite-type material $AgAlS_2$ has a direct band-edge transition close to 3.186 eV and the optical properties are similar with the Cu-based chalcopyrite-type materials. Ullah et al. [22] studied the Ag-based chalcopyrite-type material $AgXY_2$ (X = Al, Ga, In and Y = S, Se, Te) by using DFT technique. The result reveals that energy gap reduces from S to Se to Te and from Al to Ga to In. Liu et al. [23] reported that chalcopyrite-type material $AgInS_2$ is a direct band gap semiconductor with energy gap of 2.09 eV. Salehi et al. [15] stated that $AgGaX_2$ (X = S, Se, Te) chalcopyrite-type materials are direct band gap semiconductors

* Corresponding authors.
E-mail addresses: prabhat23887@gmail.com, Prabhat.ranjan@jaipur.manipal.edu (P. Ranjan), tanmoychem@gmail.com, tanmoy.chakraborty@sharda.ac.in (T. Chakraborty).

https://doi.org/10.1016/j.tsf.2020.138469
Received 3 July 2020; Received in revised form 20 November 2020; Accepted 20 November 2020
Available online 6 December 2020

and non-magnetic in nature. Kim et al. [24] reported that chalcopyrite-type material $AgInSe_2$ can be alloyed with $Cu(In,Ga)Se_2$ (CIGS) to enhance the energy gap and efficacy of CIGS thin-film photovoltaic materials.

The continuous efforts have been made by researchers in the domain of photovoltaic materials to improve its physico-chemical properties and efficiency. The Intermediate Band Solar Cell (IBSC) concept in chalcopyrite-type semiconductor has attracted a lot of attention because it helps in achieving high band gap, optical absorption and accuracy of photovoltaic cells [25–31]. In the process of IBSC, an intermediate band is sandwiched between the valence band and the conduction band. Therefore, the flow of electrons will be either from valence band to conduction band directly or from the valence band to intermediate band and then intermediate band to the conduction band. From the concept of IBSC, the performance of third generation photovoltaic cell is found nearly 87 % by placing appropriate number of intermediate bands between valence and conduction band, which is very high as compared to single-junction solar cells [28,32,33]. There are a number of reports in which it is established that titanium is the suitable transition metal to influence the realization of an intermediate band in the chalcopyrite semiconductor compound [26–29, 34–41]. Palacios et al. [38] reported that performance of photovoltaic cells is enhanced when titanium substitutes gallium in chalcopyrite-type material $CuGaS_2$. Marti et al. [29] revealed that efficiency of chalcopyrite-type material $CuGaS_2$ is enhanced after addition of Ti or Fe atom in the formation of intermediate band. The incorporation of transition metals, titanium and chromium, helps in the generation of high amount of charge carriers, which results in reduction of photon absorption energy and high accuracy for photovoltaic cells [27,35]. The solar cells with Ti-material shows the high open-circuit electric potential as well as excellent accuracy in comparison to the solar cells not having titanium material [36]. Xue et al. [42] reported that replacement of gallium by silver in compound $CuGaTe_2$ improves the performance and physicochemical properties of $CuGaTe_2$ material. The inclusion of Ag increases the carrier concentration and decreases lattice thermal conductivity which intensifies the power factor.

In this report, structure, optical and electronic properties of chalcopyrite-type material $AgTiX_2$ (X = S, Se and Te) is performed by using DFT technique. The lowest energy structure and low-lying isomers are investigated for individual clusters. The optimized lowest energy structure and low-lying isomers have real vibrational frequencies. The DFT based global descriptors viz. Highest Occupied Molecular orbital (HOMO)-Lowest Unoccupied Molecular Orbital (LUMO) energy gap, Molecular Hardness, Molecular Softness, Electronegativity, Electrophilicity Index and Dipole Moment of these materials are also studied.

2. Computational details

Density Functional Theory is considered as a computational friendly approach to solve many body problems. It has emerged as one of the most successful approaches to study aromaticity, stability and chemical reactivity of molecular systems [43–48]. We have investigated the physicochemical properties of nanoalloy clusters and chalcopyrite-type semiconductor by using DFT technique [16,49–54]. In this article, Ag-based chalcopyrite-type material $AgTiX_2$ (X = S, Se, Te) is investigated by using DFT technique. Geometry optimization and modeling for individual cluster have been done using Gaussian 03 within DFT framework [55]. Recently, Generalized Gradient Approximation (GGA) exchange correlational is reported to investigate Cu-based and Ag-based chalcopyrite-type materials [15,22,23,25,36–38]. In this study, GGA functional B3pw91 and basis set LANL2DZ are used for geometry optimization with and without 4f function on Ag with exponent of 0.45.

With the help of Koopman's Approximation, we have computed the Ionization Energy (I) and Electron Affinity (A) for chalcopyrite-type material $AgTiX_2$ (X = S, Se, Te) by using the following approach [43] -

$$I = -\varepsilon_{HOMO} \tag{1}$$

$$A = -\varepsilon_{LUMO} \tag{2}$$

The Conceptual Density Functional Theory based global descriptors viz. HOMO-LUMO energy gap, molecular hardness (η), molecular softness (S), electronegativity (χ) and electrophilicity index (ω) are also computed by using the following equations-

$$\chi = -\mu = \frac{I + A}{2} \tag{3}$$

Where, μ represents the chemical potential of the system.

$$\eta = \frac{I - A}{2} \tag{4}$$

$$S = \frac{1}{2\eta} \tag{5}$$

$$\omega = \frac{\mu^2}{2\eta} \tag{6}$$

3. Results and discussion

3.1. Geometrical structures

The lowest energy structures and isomers of $AgTiX_2$ (X = S, Se, Te) are discussed in this section and presented in Fig. 1. We have optimized various low-lying isomers during the quest for the initial structure, however six low-lying isomers optimized in the energy range of 0-2.5 eV, are presented in Fig. 1 for each cluster. For $AgTiS_2$, the lowest energy structures and its isomers are observed in the energy range of 0-2.230 eV. The rectangular structure with C_{2v} symmetry and doublet spin multiplicity is found the most suitable isomer as compared to other structures for $AgTiS_2$. The second isomer (1-b) has Y-shaped pattern with C_1 symmetry and doublet spin state. The isomer 1-b has titanium atom at the center which forms a triangle with sulfur and silver atoms and another sulfur atom is connected to this triangle. The isomer 1-b is energetically less stable than the lowest energy structure 1-a by 0.409 eV. The isomer 1-c is obtained by exchanging the position of silver and sulfur atom in isomer 1-b. The structure 1-c with C_s symmetry and spin state doublet is of higher energy than the lowest energy isomer (1-a) by 0.833 eV. The isomer 1-d has one Ag atom located at center and other atoms are attached to it, which look-alike a star-shape configuration. The isomer 1-d with C_{2v} symmetry and doublet spin is 1.250 eV less stable than the most stable structure 1-a. There is an energy difference of 0.417 eV between isomers 1-c and 1-d. The isomer 1-e is obtained by shifting Ag and Ti atom in the structure 1-b. The structure 1-e is optimized with sextet spin state and C_1 symmetry. It is 1.729 eV higher in energy than the ground state configuration 1-a. The structure 1-f is found by changing the position of Ag and Ti atoms in structure 1-c. The structure 1-f with doublet spin and C_s symmetry is less stable by 2.230 eV than the most stable structure 1-a. However, the difference in energy between structures 1-e and 1-f is 0.501 eV.

For chalcopyrite-type material $AgTiSe_2$, the lowest energy structure and its isomers are computed in the range of 0-2.416 eV. The star-shape structure with doublet spin multiplicity along with C_{2v} symmetry group is the most stable isomer (2-a). The second most stable isomer (2-b) with doublet spin state and C_{2v} symmetry has a rectangular geometry in which both the selenium atoms are lying at contrary ends. Energetically isomer 2-b is close to structure 2-a, the difference in their energy is only 0.133 eV. The isomer 2-c has a Y-shaped structure in which Ti atom is located at the center forming a triangle with both Se atoms and Ag atom is connected with the Ti atom. The isomer 2-c with C_s symmetry and spin state doublet is higher in energy (0.705 eV) than the most stable isomer (2-a). The isomers 2-d and 2-e are optimized by changing the position of

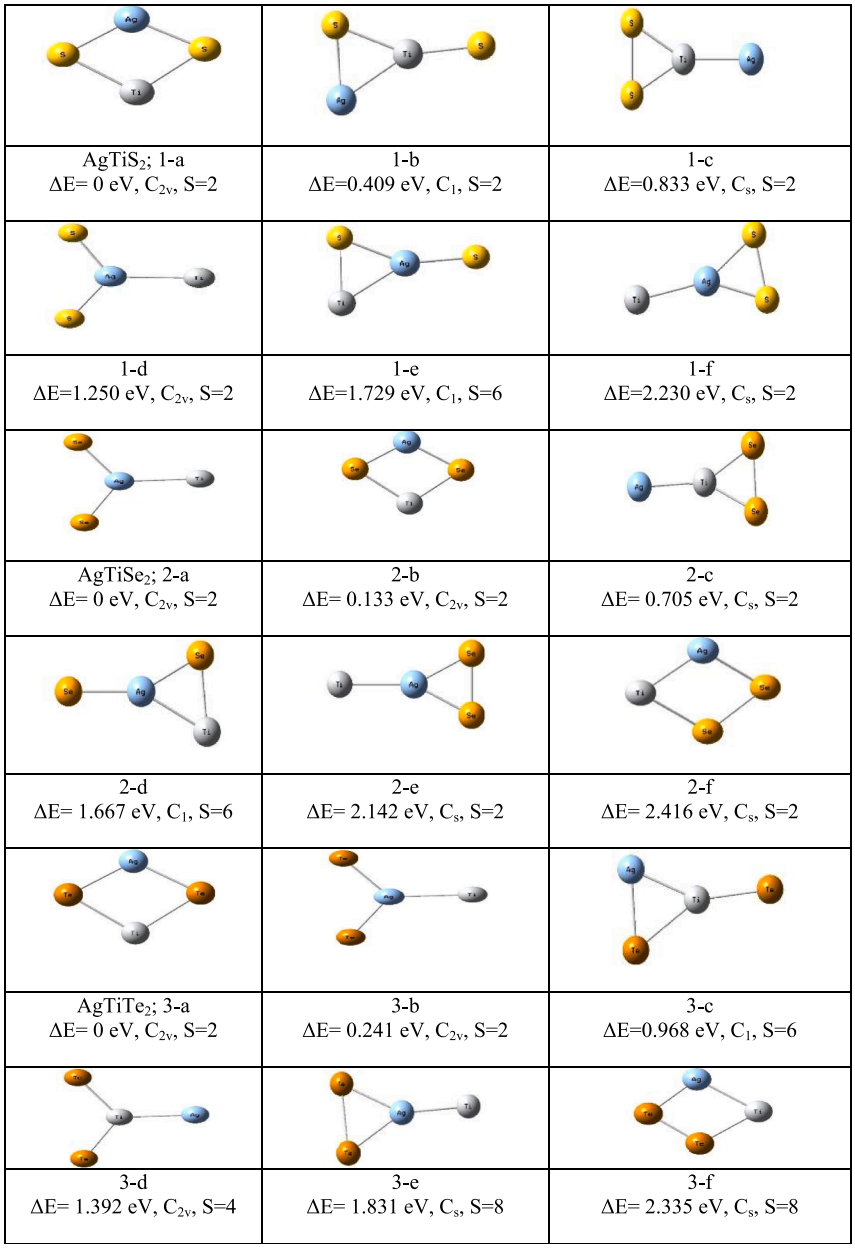

Fig. 1. Optimized structures of chalcopyrite-type material $AgTiX_2$ (X = S, Se, Te); Color legend for atoms: Ti-gray, Ag-light blue, S- yellow, Se-light yellow, Te-dark yellow. (For interpretation of the references to color in this figure legend, the reader is referred to the web version of this article.)

atoms in isomer 2-c. The isomers 2-d and 2-e are energetically higher by 1.667 eV and 2.142 eV respectively as compared to the isomer 2-a. The structure 2-f is optimized from structure 2-b by changing the position of sulfur and titanium atoms. The structure 2-f with Cs symmetry and spin state doublet is less stable than the lowest energy structure (2-a) by 2.416 eV. The isomer 2-f is 0.274 eV higher in energy only than the isomer 2-e.

For $AgTiTe_2$, the lowest energy structure and its isomers are optimized in the range of 0-2.335 eV. The rectangular shape geometry with doublet spin multiplicity and C_{2v} symmetry is the most stable isomer (3-a). The second isomer (3-b) has one Ag atom at the center and other atoms are directly joined to silver atom, which form a star-like configuration. The isomer 3-b with C_{2v} symmetry group and doublet spin multiplicity is energetically higher by 0.241 eV in comparison to the lowest energy isomer (3-a). The structure 3-c with Y-shaped structure has a Ti atom at the center which forms a triangle with Te and Ag atoms. The isomer 3-c with sextet spin state and C_1 symmetry is less stable by 0.968 eV than the isomer 3-a. The isomer 3-d is optimized from structure 3-b by swapping the position of silver and titanium atom. The structure 3-d with symmetry group C_{2v} and quartet spin multiplicity is 1.392 eV higher in energy than the most stable structure 3-a. The difference in energy between isomers 3-c and 3-d is found as 0.424 eV. The isomers 3-e and 3-f are optimized from structures 3-c and 3-a respectively. Both the isomers have Cs symmetry group and octet spin multiplicity. The structures 3-e and 3-f are energetically less stable than the initial structure of compound $AgTiTe_2$ by 1.831 eV and 2.335 eV respectively. However, difference in energy found between isomers 3-e and 3-f are 0.504 eV.

3.2. Optical properties

In this section, harmonic frequencies, IR activities and Raman scattering activities of chalcopyrite-type material $AgTiX_2$ (X = S, Se, Te) are computed through B3pw91/LANL2DZ within DFT framework. The

Raman and IR spectra of these materials are shown in Figs. 2 and 3 respectively. For $AgTiS_2$, several IR and the Raman peaks are observed in the frequency range of 0–493.26 cm^{-1} (wave number unit). The highest value of IR spectra (122.255 km/mole) is located at the maximum frequency, whereas the peak at Raman spectra (48.945 a.u.) is found at harmonic frequency 447.509 cm^{-1}. The lowest intensity of IR (0.55 km/mole) and Raman (4.224 a.u.) spectra is observed at frequencies 178.973 cm^{-1} and 493.265 cm^{-1} respectively.

The Raman and IR spectra for chalcopyrite-type material $AgTiSe_2$ are found in the range of 0-371.99 cm^{-1}. At the maximum vibrational frequency, we have observed the peak value of IR spectra i.e. 75.132 km/mole, whereas the IR spectra with lowest intensity is found at 128.688 cm^{-1}. The peak value of Raman spectra (44.660 a.u.) is observed at 310.251 cm^{-1}. The Raman spectra with very less intensity (0.227 a.u.) is found at frequency 70.9992 cm^{-1}.

The Raman and IR spectra for $AgTiTe_2$ are observed in the range of 0-248.796 cm^{-1}. The maximum value of IR spectra (12.520 km/mole) and

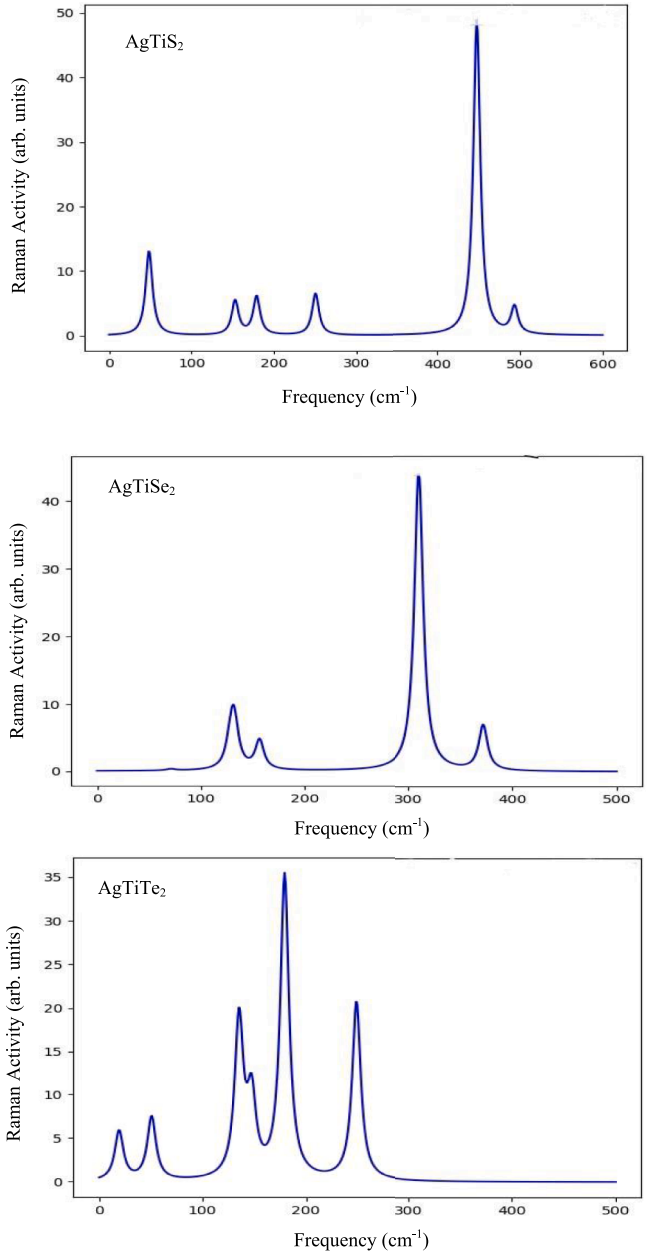

Fig. 2. The Raman activity of chalcopyrite-type material $AgTiX_2$ (X = S, Se, Te)

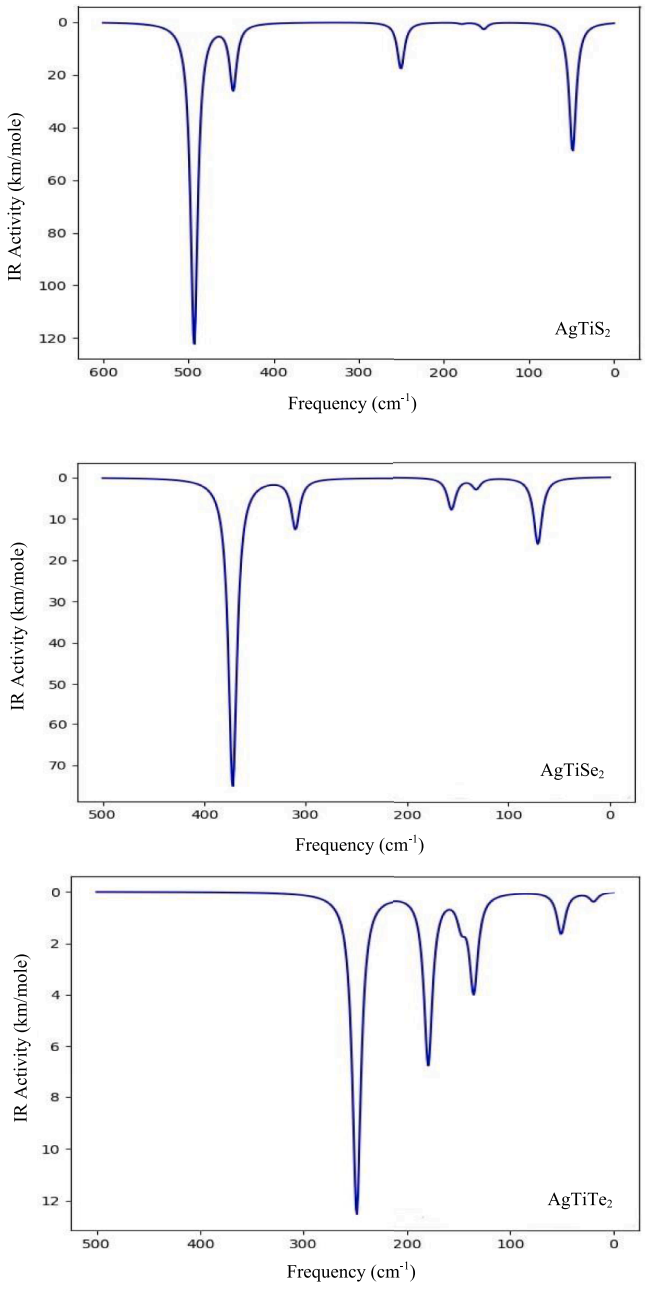

Fig. 3. The IR activity of chalcopyrite-type material $AgTiX_2$ (X = S, Se, Te)

Raman spectra (34.953 a.u.) is found at harmonic frequency 248.796 cm^{-1} and 179.387 cm^{-1} respectively. However, at frequency 19.391 cm^{-1}, the least value of Raman and IR intensity is marked.

The Raman and IR spectra shows that the maximum range of harmonic frequencies and peak intensities of IR and Raman spectra are observed for compound $AgTiS_2$, whereas $AgTiTe_2$ have the least value. The harmonic frequency and intensity of IR and Raman spectra decreases from compound $AgTiS_2$ to $AgTiSe_2$ to $AgTiTe_2$. It is based on the concept that these properties are related to the flow of electrons as band gap of these chalcopyrite-type materials deceases when it moves from S to Se to Te [22].

3.3. *Electronic properties and DFT based descriptors*

The electronic properties and density functional theory based global descriptors of Ag-based chalcopyrite compounds $AgTiX_2$ (X = S, Se, Te)

are studied in this section. In his seminal work, Fukui established that the source of charge transfers and technique of dealings of molecular orbitals of donor and acceptor become distinct and clear in the electronic structure method of donor-acceptor system [56,57]. The study suggests that the frontier orbitals, the Highest Occupied Molecular orbital (HOMO) and the Lowest Unoccupied Molecular Orbital (LUMO) of donor and acceptor, have significant involvement in transfer of charge and bonding in the establishment of donor-acceptor molecular system [56–59]. There is a concurrent method of contribution from the donor HOMO to the acceptor LUMO and then afterwards reverse contribution to the LUMO of the donor from the acceptor HOMO. It shows the entire process for the development of donor-acceptor in a molecular system [56,57]. The energy difference between HOMO and LUMO is a significant tool to investigate the electronic stability of chalcopyrite semiconductors. It signifies the required lowest energy to excite the electrons from valence band to conduction band [58].

The DFT based global descriptors and dipole moment of chalcopyrite-type material $AgTiX_2$ (X = S, Se, Te) computed using B3pw91/LANL2DZ with and without 4f function on Ag with exponent of 0.45 are presented in Tables 1 and 2 respectively. The result shows that HOMO-LUMO energy gap with 4f function on Ag varies from 2.319 eV-3.211 eV whereas without 4f function on Ag varies between 2.092 eV-3.056 eV. This value is in well agreement with the energy gap required for optoelectronic and photovoltaic devices especially for solar cell applications. Karaagac et al. [59] reported that energy gap for compound $AgGaS_2$ is in the range of 2.30–2.75 eV. Previous studies also show that band gaps for Ag-based chalcopyrite-type materials like $AgAlX_2$, $AgGaX_2$, $AgInX_2$ (X = S, Se, Te) vary from 2.35 eV to 3.60 eV, 1.1 eV to 2.70 eV and 0.93 eV to 1.9 eV respectively [15,22,58]. The calculated HOMO-LUMO energy gap is in agreement with the available experimental data for Ag-based chalcopyrite compounds [58,59]. The previous data shows that energy gap along with performance of photovoltaic cell is enhanced after incorporation of titanium in chalcopyrite compound [25–27,29,34–41]. The system without 4f function on Ag display less value of HOMO-LUMO energy gap as compared to the system with 4f function on Ag. It is noted from Tables 1 and 2 that HOMO-LUMO energy gap follow the order as $AgTiS_2 > AgTiSe_2 > AgTiTe_2$. It shows that HOMO-LUMO gap decreases in the order of S to Se to Te, which is in line with the previous studies reported by Ullah et al. [22] and Xiao et al. [58] for Ag-based chalcopyrite-type materials and Zhou et al. [60] for Cu-based chalcopyrite-type material. Importance of the band gap to determine the resultant transfer of charge through the interface between donor and acceptor of any molecular system is already distinct through previous scientific reports [61–63].

From the computed data, we can observe that DFT based global descriptors molecular hardness, electronegativity and electrophilicity index have a linear relationship with HOMO-LUMO energy gap. Similarly, HOMO-LUMO energy gap of these compounds have an inverse relationship with molecular softness. It means that chalcopyrite compound with maximum energy gap is more stable and vice-versa. The result shows that system with 4f function on Ag have larger value of molecular hardness as compared to the system without 4f function on Ag. The molecular hardness for both the system follows the trend i.e. $AgTiS_2 > AgTiSe_2 > AgTiTe_2$. It shows that molecular hardness decreases from S to Se to Te. For system with 4f function on Ag, $AgTiS_2$ displays the maximum value of molecular hardness (1.606 eV) whereas $AgTiTe_2$ shows the minimum value (1.159 eV). Similarly, for system without 4f function on Ag, $AgTiS_2$ and $AgTiTe_2$ exhibits the maximum and minimum hardness value respectively. From the above result, it is clear that chalcopyrite-material $AgTiS_2$ is the most stable whereas $AgTiTe_2$ is the least stable system.

The result shows that system with 4f function on Ag have smaller value of molecular softness as compared to the system without 4f function on Ag. Molecular softness for chalcopyrite-type material $AgTiX_2$ exhibits trend i.e. $AgTiTe_2 > AgTiSe_2 > AgTiS_2$. It indicates that molecular softness increases from S to Se to Te. For system with 4f function on Ag, $AgTiTe_2$ shows the maximum softness value as 0.431 eV whereas $AgTiS_2$ displays the minimum value as 0.311 eV. Similarly, for system without 4f function on Ag, $AgTiTe_2$ and $AgTiS_2$ shows the maximum and minimum value of molecular softness as 0.478 eV and 0.327 eV respectively.

Sanderson [64] defined electronegativity equalization as “When two species come together, electrons start moving from lower electronegativity to higher electronegativity species. This process will continue until electronegativity of all the systems i.e. donor, acceptor and adduct will become static at some level [56].” Chalcopyrite-type material $AgTiX_2$ with 4f function on Ag have larger value of electronegativity as compared to the system without 4f function on Ag. The electronegativity follows the order i.e. $AgTiS_2 > AgTiSe_2 > AgTiTe_2$.

The electrophilicity index of compound is dependent on the ionization energy and electron affinity [44]. It specifies the amount of energy lowering for a compound due to extensive flow of electron during the interaction between donor and acceptor. The electrophilicity index for chalcopyrite-type material $AgTiX_2$ without 4f function on Ag is found more as compared to the system without 4f function on Ag. The electrophilicity index follows the order i. e. $AgTiS_2 > AgTiSe_2 > AgTiTe_2$. It indicates that value of electrophilicity index decreases from S to Se to Te. For system without 4f function on Ag, the maximum value of electrophilicity index is observed for compound $AgTiS_2$ i.e. 9.577 eV whereas, $AgTiTe_2$ has the lowest value i.e. 7.466 eV. However, for system without 4f function on Ag, $AgTiS_2$ and $AgTiTe_2$ exhibits the maximum and minimum value of electrophilicity index as 0.335 eV and 0.260 eV respectively.

The dipole moment (in Debye) for $AgTiX_2$ follows the trend i.e. $AgTiTe_2 > AgTiSe_2 > AgTiS_2$. For system with 4f function on Ag, $AgTiS_2$ and $AgTiTe_2$ exhibits the minimum and maximum value i.e. 0.477 Debye and 1.988 Debye respectively. Similarly, for system without 4f function on Ag, minimum and maximum values are obtained for $AgTiS_2$

Table 1
DFT based descriptors of chalcopyrite-type material $AgTiX_2$ (X = S, Se, Te) with 4f function on Ag.

Compound	HOMO-LUMO Energy Gap (eV)	Hardness (eV)	Softness (eV)	Electronegativity (eV)	Electrophilicity Index (eV)	Dipole Moment (Debye)
$AgTiS_2$	3.211	1.606	0.311	0.914	0.335	0.477
$AgTiSe_2$	2.477	1.239	0.404	0.887	0.318	1.885
$AgTiTe_2$	2.319	1.159	0.431	0.881	0.260	1.988

Table 2
DFT based descriptors of chalcopyrite-type material $AgTiX_2$ (X = S, Se, Te) without 4f function on Ag.

Compound	HOMO-LUMO Energy Gap (eV)	Hardness (eV)	Softness (eV)	Electronegativity (eV)	Electrophilicity Index (eV)	Dipole Moment (Debye)
$AgTiS_2$	3.056	1.528	0.327	4.777	9.577	0.945
$AgTiSe_2$	2.411	1.205	0.415	4.751	9.365	0.949
$AgTiTe_2$	2.092	1.046	0.478	4.476	7.466	5.295

and $AgTiTe_2$ i.e. 0.945 Debye and 5.295 Debye respectively.

For chalcopyrite-type material $AgTiS_2$, our calculated bond lengths between Ti-S, Ag-Ti and Ag-S are 2.21 Å, 2.89 Å, 2.602 Å respectively. Liu et al. [23] investigated that for chalcopyrite-type material $AgInS_2$, the experimental and theoretical bond length between Ag-S is 2.56 Å and 2.58 Å respectively. For compound $AgTiSe_2$, the calculated bond lengths between Ti-Se, Ag-Ti and Ag-Se are 2.36 Å, 2.862 Å, 2.695 Å respectively. In the case of $AgTiTe_2$, the computed bond lengths between Ti-Te, Ag-Ti, Ag-Te are 2.72 Å, 2.715 Å, 3.121 Å respectively. Salehi et al. [15] reported that for chalcopyrite-type material $AgGaX_2$ (X = S, Se, Te), the bond lengths are in the order of Ag-Te > Ag-Se > Ag-S. Our computed bond lengths for $AgTiX_2$ (X=S, Se, Te) also follow the same order.

4. Conclusion

Structures along with electronic and optical properties of Ag-based chalcopyrite-type semiconductor material $AgTiX_2$ (X = S, Se, Te) are studied in terms of density functional theory methodology. The lowest energy structure shows that HOMO-LUMO energy gap of $AgTiX_2$ with and without 4f function on Ag is in the range of 2.319 eV – 3.211 eV and 2.092 eV – 3.056 eV respectively. This particular energy level is suitable for optoelectronic and photovoltaic devices especially for solar cell applications. The chalcopyrite-type material $AgTiS_2$, with C_{2v} symmetry group and doublet spin multiplicity, is energetically more stable than the other similar type of molecules. Our computed result reveals that HOMO-LUMO energy gap, harmonic frequency and intensity of IR and Raman spectra decreases from compound $AgTiS_2$ to $AgTiSe_2$ to $AgTiTe_2$. DFT based global descriptors of these chalcopyrite-type materials establishes a strong relationship with HOMO-LUMO energy gap of the respective molecules.

Data Availability Statement

"The proposed study required to reproduce these findings cannot be shared at this time as the data also forms part of an ongoing study".

CRediT authorship contribution statement

Prabhat Ranjan: Conceptualization, Data curation, Investigation, Methodology, Resources, Software, Writing - original draft. **Pancham Kumar:** Conceptualization, Investigation. **Praveen K. Surolia:** Formal analysis, Validation. **Tanmoy Chakraborty:** Project administration, Visualization, Writing - review & editing.

Declaration of Competing Interest

The authors declare that they have no known competing financial interests or personal relationships that could have appeared to influence the work reported in this paper.

Acknowledgement

Dr Tanmoy Chakraborty and Dr Prabhat Ranjan are thankful to Sharda University and Manipal University Jaipur respectively for providing research support and computational facilities.

References

[1] C.H. Ho, C.C. Pan, Surface sensing behavior and band edge properties of $AgAiS_2$: experimental observations in optical, chemical, and thermoreflectance spectroscopy, AIP Adv. 2 (2012), 022123. https://doi.org/10.1063/1.4718342.
[2] M.G. Panthani, V. Akhavan, B. Goodfellow, J.P. Schmidtke, L. Dunn, A. Dodabalapur, P.F. Barbaba, B.A. Korgel, Synthesis of $CuInS_2$, $CuInSe_2$ and $Cu(In_xGa_{1-x})Se_2$ (CIGS) nanocrystal "lnks" for printable photovoltaics, J. Am. Chem. Soc. 130 (2008) 16770–16777. https://doi.org/10.1021/ja805845q.
[3] N. Naghavi, S. Spiering, M. Powalla, B. Cavana, D. Lincot, High-efficiency copper indium gallium diselenide (CIGS) solar cells with indium sulfide buffer layers deposited by atomic layer chemical vapor deposition (ALCVD), Prog. Photovolt. 11 (2003) 437–443. https://doi.org/10.1002/pip.508.
[4] M.L.A. Aguilera, J.R.A. Hernandez, M.A.G. Trujillo, M.O. Lopez, Photoluminescence studies of p-type chalcopyrite $AgInS_2$: Sn, Sol. Energy Mater. Sol. Cells 91 (2007) 1483–1487. https://doi.org/10.1016/j.solmat.2007.05.006.
[5] S. Chichibu, H. Nakanishi, S. Shirakata, Ultraviolet photoluminescence from $CuAlS_2$ heteroepitaxial layers grown by low-pressure metalorganic chemical vapor deposition, Appl. Phys. Lett. 66 (1995) 3513. https://doi.org/10.1063/1.113781.
[6] S.T. Cornor, C.M. Hsu, B.D. Weil, S. Aloni, Y. Cui, Phase transformation of biphasic Cu_2S-$CuInS_2$ to monophasic $CuInS_2$ nanorods, J. Am. Chem. Soc. 131 (2009) 4962–4966. https://doi.org/10.1021/ja809901u.
[7] C.H. Ho, Thermoreflectance characterization of band-edge excitonic transitions in $CuAiS_2$ ultraviolet solar-cell materials, Appl. Phys. Lett. 96 (2010), 061902. https://doi.org/10.1063/1.3303826.
[8] I. Tsuji, H. Kato, A. Kudo, Visible-light-induced H2 evolution from an aqueous solution containing sulfide and sulfite over a ZnS-$CuInS_2$-$AgInS_2$ solid-solution photocatalyst, Angew. Chem. Int. Ed. 44 (2005) 3631–3634. https://doi.org/10.1002/ange.200500314.
[9] I. Tsuji, H. Kato, H. Kobayashi, A. Kudo, Photocatalytic H2 evolution reaction from aqueous solutions over band structure-controlled $(AgIn)_xZn_{2(1-x)}S_2$ solid solution photocatalysts with visible-light response and their surface nanostructures, J. Am. Chem. Soc. 126 (2004) 13406–13413. https://doi.org/10.1021/ja048296m.
[10] V.V. Badikov, O.N. Pivovarov, Y.V. Skokov, O.V. Skrebneva, N.K. Trotsenko, Some optical properties of silver thiogallate single crystals, Sov. J. Quantum Electron. 5 (1975) 350–351. https://doi.org/10.1070/QE1975v005n03ABEH011027.
[11] F.C. Akkari, R. Brini, M. Kanzari, B. Rezig, High absorbing $CuInS_2$ thin films growing by oblique angle incidence deposition in presence of thermal gradient, J. Mater. Sci. 40 (2005) 5751–5755. https://doi.org/10.1007/s10853-005-1134-5.
[12] B. Mao, C.H. Chung, J. Wang, C. Burda, Synthesis and photophysical properties of ternary I-III-VI $AgInS_2$ nanocrystals: Intrinsic versus surface states, J. Phys. Chem. C 115 (2011) 8945–8954. https://doi.org/10.1021/jp2011183.
[13] Y. Hamanaka, T. Ogawa, M. Tsuzuki, T. Kuzuya, Photoluminescence properties and its origin of $AgInS_2$ quantum dots with chalcopyrite structure, J. Phys. Chem. C 115 (2011) 1786–1792. https://doi.org/10.1021/jp110409q.
[14] H. Karaagac, Electrical, structural and optical properties of AgGaSe2-xSx thin films grown by sintered powder, PhD Thesis, Middle East Technical University, Ankara, Turkey, 2010.
[15] H. Salehi, E. Gordanian, Ab initio study of structural, electronic and optical properties of ternary chalcopyrite semiconductors, Mater. Sci. Semicond. Process. 47 (2016) 51–56. https://doi.org/10.1016/j.mssp.2016.02.015.
[16] P. Ranjan, P. Kumar, T. Chakraborty, M. Sharma, S. Sharma, A study of structure and electronic properties of chalcopyrites semiconductor invoking density functional theory, Mater. Chem. Phys. 241 (2020), 122346. https://doi.org/10.1016/j.matchemphys.2019.122346.
[17] H. Karaagac, M. Kaleli, M. Parlak, Characterization of $AgGa_{0.5}In_{0.5}Se_2$ thin films deposited by electron-beam technique, J. Phys. D: Appl. Phys. 42 (2009) 165413–165419. https://doi.org/10.1088/0022-3727/42/16/165413.
[18] H.-C. Hsu, H.-H. Chen, S.Y. Kuo, C.-S. Chang, W.-F. Hsieh, Effect of annealing on the structural and optical properties of $AgGaS_2$ thin films prepared by pulsed laser deposition, Thin Solid Films 419 (2002) 237–241. https://doi.org/10.1016/S0040-6090(02)00743-5.
[19] C. Merschjann, M. Mews, T. Mete, A. karkatzinou, M. Rusu, B.V. Korzun, S. Schorr, P. Schubert-Bischoff, S. Seeger, T. Schedel-Niedrig, M.-C. Lux-Steiner, $AgGaSe_2$ thin films grown by chemical close-spaced vapor transport for photovoltaic applications: structural, compositional and optical properties, J. Phys. 24 (2012) 175801–175810. https://doi.org/10.1088/0953-8984/24/17/175801.
[20] O. Aissaoui, S. Mehdaoui, L. Bechiri, M. Benabdeslem, N. Benslim, A. Amara, L. Mahdjoubi, G. Nouet, Synthesis and material properties of Cu-III-VI_2 chalcopyrite thin films, J. Phys. D 40 (2007) 5663–5665. https://doi.org/10.1088/0022-3727/40/18/021.
[21] S.H. You, K.J. Hong, B.J. Lee, T.S. Jeong, C.J. Youn, J.S. Park, S.N. Baek, Temperature dependence of band gap and photocurrent properties for the $AgInS_2$ epilayers grown by hot wall epitaxy, J. Cryst. Growth 245 (2002) 261–266. https://doi.org/10.1016/S0022-0248(02)01729-3.
[22] S. Ullah, H.U. Din, G. Murtaza, T. Ouahrani, R. Khenata, S. Naeemullah, B. Omran, Structure, electronic and optical properties of $AgXY_2$ (X=Al, Ga, In and Y= S, Se, Te), J. Alloys Compd 617 (2014) 575–583. https://doi.org/10.1016/j.jallcom.2014.08.058.
[23] J. Liu, S. Chen, Q. Liu, Y. Zhu, Y. Lu, Density functional theory study on electronic and photocatalytic properties of orthorhombic $AgInS_2$, Comput. Mater. Sci. 91 (2014) 159–164. https://doi.org/10.1016/j.commatsci.2014.05.010.
[24] N. Kim, P.P. Martin, A.A. Rockett, E. Ertekin, First-principle study of the electronic structure and stability of reconstructed $AgInSe_2$ (112) polar surfaces, IEEE J. Photovolt. 7 (2017) 1781–1788, https://doi.org/10.1109/JPHOTOV.2017.2754061.
[25] I. Aguilera, P. Palacios, P. Wahnon, Optical properties of chalcopyrite-type intermediate transition metal band materials from first principles, Thin Solid Films 516 (2008) 7055–7059. https://doi.org/10.1016/j.tsf.2007.12.085.
[26] I. Aguilera, P. Palacios, P. Wahnon, Enhancement of optical absorption in Ga-chalcopyrite-based intermediate-band materials for high efficiency solar cells, Sol. Energy Mater. Sol. Cells 94 (2010) 1903–1906. https://doi.org/10.1016/j.solmat.2010.06.019.
[27] P. Chen, M. Qin, H. Chen, C. Yang, Y. Wang, F. Huang, Cr incorporation in $CuGaS_2$ chalcopyrite: a new intermediate-band photovoltaic materials with wide-spectrum absorption, Phys. Stat. Sol. 210 (2013) 1098–1102. https://doi.org/10.1002/pssa.201228721.

[28] T. Wang, X. Li, W. Li, L. Huang, C. Ma, Y. Cheng, J. Cui, H. Luo, G. Zhong, C. Yang, Transitions metals doped $CuAlSe_2$ for promising intermediate band materials, Mater. Res. Express. 3 (2016), 045905. https://doi.org/10.1088/2053-1591/3/4/045905.

[29] A. Marti, D.F. Marron, A. Luque, Evaluation of the efficiency potential of intermediate band solar cells based on thin-film chalcopyrite materials, J. Appl. Phys. 103 (2008), 073706. https://doi.org/10.1063/1.2901213.

[30] W. Wang, A.S. Lin, J.D. Phillips, Intermediate-band photovoltaic solar cell based on ZnTe:O, Appl. Phys. Lett. 95 (2009), 011103. https://doi.org/10.1063/1.3166863.

[31] S. Siebentritt, Chalcopyrite compound semiconductors for thin film solar cells, Curr. Opin. Green Sustain. Chem. 4 (2017) 1–7. https://doi.org/10.1016/j.cogsc.2017.02.001.

[32] M.A. Green, Third generation photovoltaics: ultra-high conversion efficiency at low cost, Prog. Photovolt. 9 (2001) 123–135. https://doi.org/10.1002/pip.360.

[33] T. Nozawa, Y. Arakawa, Detailed balance limit of the efficiency of multilevel intermediate band solar cells, Appl. Phys. Lett. 98 (2011) 171108–171111. https://doi.org/10.1063/1.3583587.

[34] C. Tablero, Ionization levels of doped sulfur and selenium chalcopyrites, J. Appl. Phys. 106 (2009), 073718. https://doi.org/10.1063/1.3243336.

[35] X. Lv, S. Yang, M. Li, H. Li, J. Yi, M. Wang, G. Niu, J. Zhong, Investigation of a novel intermediate band photovoltaic material with wide spectrum solar absorption based on Ti-substituted $CuGaS_2$, Solar Energy 103 (2014) 480–487. https://doi.org/10.1016/j.solener.2014.02.046.

[36] B. Marsen, L. Steinkopf, A. Singh, H. Wilhelm, I. Lauermann, T. Unold, R. Scheer, H.W. Schock, Effect of Ti-incorporation in $CuInS_2$ solar cells, Sol. Energy Mater. Sol. Cells 94 (2010) 1730–1733. https://doi.org/10.1016/j.solmat.2010.05.036.

[37] K. Hashikuni, K. Suekuni, H. Usui, R. Chetty, M. Ohta, K. Kuroki, T. Takabatake, K. Watanabe, M. Ohtaki, Thermoelectric properties and electronic structures of $CuTi_2S_4$ thiospinel and its derivatives: structural design for spinel-related thermoelectric materials, Inorg. Chem. 58 (2019) 1425–1432. https://doi.org/10.1021/acs.inorgchem.8b02955.

[38] P. Palacios, K. Sanchez, J.C. Conesa, P. Wahnon, First principles calculation of isolated intermediate bands formation in a transition metal-doped chalcopyrite-type semiconductor, Phys. Stat. Sol. 203 (2006) 1395–1401. https://doi.org/10.1002/pssa.200566179.

[39] P. Palacios, K. Sanchez, J.C. Conesa, J.J. Fernandez, P. Wahnon, Theoretical modelling of intermediate band solar cell materials based on metal-doped chalcopyrite compounds, Thin Solid Films 515 (2007) 6280–6284. https://doi.org/10.1016/j.tsf.2006.12.170.

[40] P. Palacios, P. Wahnon, S. Pizzinato, J.C. Conesa, Energetics of formation of $TiGa_3As_4$ and $TiGa_3P_4$ intermediate band materials, J. Chem. Phys. 124 (2006), 014711. https://doi.org/10.1063/1.2140695.

[41] P. Palacios, I. Aguilera, P. Wahnon, J.C. Conesa, Thermodynamics of the formation of Ti- and Cr-doped $CuGaS_2$ intermediate-band photovoltaic materials, J. Phys. Chem. C 112 (2008) 9525–9529. https://doi.org/10.1021/jp0774185.

[42] L. Xue, B. Xu, D. Zhao, L. Yi, First-principle calculations of the electronic, elastic and thermoelectric properties of Ag doped $CuGaTe_2$, Intermetallics 55 (2014) 204–209. https://doi.org/10.1016/j.intermet.2014.08.005.

[43] R.G. Parr, W. Yang, Density functional theory of atoms and molecules, Oxford University Press, Oxford, 1989.

[44] P.K. Chattaraj, U. Sarkar, D.R. Roy, Electrophilicity Index, Chem. Rev. 106 (2006) 2065–2091. https://doi.org/10.1021/cr040109f.

[45] R. Parthasarathi, J. Padmanabhan, M. Elango, K. Chitra, V. Subramanian, P. K. Chattaraj, pK prediction using group philicity, J. Phys. Chem. A 110 (2006) 6540–6544. https://doi.org/10.1021/jp055849m.

[46] E. Chamorro, P.K. Chattaraj, P. Fuentealba, Variation of the electrophilicity index along the reaction path, J. Phys. Chem. A 107 (2003) 7068–7072. https://doi.org/10.1021/jp035435y.

[47] R. Parthasarathi, M. Elango, V. Subramanian, P.K. Chattaraj, Variation of electrophilicity during molecular vibrations and internal rotations, Theor. Chem. Accounts 113 (2005) 257–266. https://doi.org/10.1007/s00214-005-0634-3.

[48] S. Pan, M. Sola, P.K. Chattaraj, On the validity of the maximum hardness principle and the minimum electrophilicity principle during chemical reactions, J. Phys. Chem. 117 (2013) 1843–1852. https://doi.org/10.1021/jp312750n.

[49] P. Ranjan, T. Chakraborty, Density functional approach: to study copper sulfide nanoalloy clusters, Acta Chim. Slov. 66 (2019) 173–181. https://doi.org/10.17344/acsi.2018.4762.

[50] P. Ranjan, S. Dhail, S. Venigalla, A. Kumar, L. Ledwani, T. Chakraborty, A theoretical analysis of bi-metallic $(CuAg)_{n=1-7}$ nano alloy clusters invoking DFT based descriptors, Mat. Sci.- Pol. 33 (2016) 719–724, 2016, https://doi.org/10.1515/msp-2015-0121.

[51] P. Ranjan, T. Chakraborty, A. Kumar, Computational study of Au doped Cu nano alloy clusters, Nano Hybrids 17 (2017) 62–71. https://doi.org/10.4028/www.scientific.net/NHC.17.62.

[52] P. Ranjan, T. Chakraborty, A. Kumar, Computational investigation of cationic, anionic and neutral Ag_2Au_N (N=1-7) nanoalloy clusters, Phys. Sci. Rev. 2 (2017), 2016012. https://doi.org/10.1515/psr-2016-0112.

[53] P. Ranjan, T. Chakraborty, A DFT study of vanadium doped gold nanoalloy clusters, Key Eng. Mater. 77 (2018) 183–189. https://doi.org/10.4028/www.scientific.net/KEM.777.183.

[54] P. Ranjan, T. Chakraborty, A comparative study of structure, stabilities and electronic properties of neutral and cationic $[AuSi_n]^{\lambda}$ and $[Si_{n+1}]^{\lambda}$ (λ=0, +1; n=1-12) nanoalloy clusters, Mat. Today Commun. 22 (2020), 100832. https://doi.org/10.1016/j.mtcomm.2019.100832.

[55] M.J. Frisch, G.W. Trucks, H.B. Schlegel, G.E. Scuseria, M.A. Robb, J.R. Cheeseman, J.A. Montgomery Jr, T. Vreven, K.N. Kudin, J.C. Burant, J.M. Millam, S.S. Iyengar, J. Tomasi, V. Barone, B. Mennucci, M. Cossi, G. Scalmani, N. Rega, G.A. Petersson, H. Nakatsuji, M. Hada, M. Ehara, K. Toyota, R. Fukuda, J. Hasegawa, M. Ishida, T. Nakajima, Y. Honda, O. Kitao, H. Nakai, M. Klene, X. Li, J.E. Knox, H. P. Hratchian, J.B. Cross, V. Bakken, C. Adamo, J. Jaramillo, R. Gomperts, R. E. Stratmann, O. Yazyev, A.J. Austin, R. Cammi, C. Pomelli, J.W. Ochterski, P. Y. Ayala, K. Morokuma, G.A. Voth, P. Salvador, J.J. Dannenberg, V.G. Zakrzewski, S. Dapprich, A.D. Daniels, M.C. Strain, O. Farkas, D.K. Malick, A.D. Rabuck, K. Raghavachari, J.B. Foresman, J.V. Ortiz, Q. Cui, A.G. Baboul, S. Clifford, J. Cioslowski, B.B. Stefanov, G. Liu, A. Liashenko, P. Piskorz, I. Komaromi, R. L. Martin, D.J. Fox, T. Keith, M.A. Al-Laham, C.Y. Peng, A. Nanayakkara, M. Challacombe, P.M.W. Gill, B. Johnson, W. Chen, M.W. Wong, C. Gonzalez, J. A. Pople, Gaussian 03, Revision C.02, Gaussian, Inc., Wallingford CT, 2004.

[56] H. Fujimoto, S. Kato, S. Yamabe, K. Fukui, Molecular orbital calculations of the electronic structure of borazane, J. Chem. Phys. 60 (1974) 572–578. https://doi.org/10.1063/1.1681075.

[57] D.C. Ghosh, S. Bhattacharyya, Molecular orbital and density functional study of the formation, charge transfer, bonding and the conformational isomerism of the boron trifluoride (BF3) and ammonia (NH3) donor-acceptor complex, Int. J. Mol. Sci. 5 (2004) 239–264. https://doi.org/10.3390/i5050239.

[58] H. Xiao, J.T. Kheli, W.A. Goddard III, Accurate band gaps for semiconductors from density functional theory, J. Phys. Chem. Lett. 2 (2011) 212–217. https://doi.org/10.1021/jz101565j.

[59] H. Karaagac, M. Parlak, The investigation of structural, electrical and optical properties of thermal evaporated AgGaS2 thin films, Thin Solid Films 519 (2011) 2055–2061. https://doi.org/10.1016/j.tsf.2010.10.027.

[60] H.G. Zhou, H. Chen, D. Chen, Y. Li, K.N. Ding, X. Huang, Y.F. Zhang, Electronic structures and optical properties of $CuAlX_2$ (X= S, Se, te) semiconductors with a chalcopyrite structure, Acta Phys. Chim. Sin. 27 (2011) 2805–2813, https://doi.org/10.3866/PKU.WHXB20112805.

[61] D.C. Ghosh, J. Jana, Frontier orbital and density functional study of the variation of the hard-soft behavior of monoborane (BH_3) and boron trifluoride (BF_3) as a function of angles of reorganization from planar (D_{3h}) to pyramidal (C_{3v}) shape, Int. J. Quant. Chem. 92 (2003) 484–505. https://doi.org/10.1002/qua.10482.

[62] Z. Zhou, R.G. Parr, Activation hardness: new index for describing the orientation of electrophile aromatic substitution, J. Am. Chem. Soc. 112 (1990) 5720–5724. https://doi.org/10.1021/ja00171a007.

[63] R.G. Parr, Z. Zhou, Absolute hardness: unifying concept for identifying shells and subshells in nuclei, atoms, molecules and metallic clusters, Acc. Chem. Res. 26 (1993) 256–258. https://doi.org/10.1021/ar00029a005.

[64] R.T. Sanderson, Electronegativities in inorganic chemistry, J. Chem. Ed. 29 (1952) 539. https://doi.org/10.1021/ed029p539.